Steel and Composite Structures, *Vol. 26, No. 3 (2018) 289-301*
DOI: https://doi.org/10.12989/scs.2018.26.3.289

Seismic behavior of beam-to-column connections with elliptic slit dampers

Saeed Farahi Shahri [a] and Seyed Roohollah Mousavi [*]

Civil Engineering Department, University of Sistan and Baluchestan, Daneshgah Street, Zahedan 98155-987, Iran

(*Received January 8, 2017, Revised July 29, 2017, Accepted October 24, 2017*)

Abstract. The rigid steel connections were suffered severe damage because of low rotational capacity during earthquakes. Hence, many investigations have been conducted on the connections of steel structures. As a solution, steel slit dampers were employed at the connections to prevent brittle failure of connections and damage of main structural members. Slit damper is a plate or a standard section with a number of slits in the web. The objective of this paper is to improve the seismic performance of steel slit dampers in the beam-to-column connection using finite element modeling. With reviewing the previous investigations, it is observed that slit dampers were commonly fractured in the end parts of the struts. This may be due to the low participation of struts middle parts in the energy dissipation. Thus, in the present study slit damper with elliptic slits is proposed in such a way that end parts of struts have more energy absorption area than struts middle parts. A parametric study is conducted to investigate the effects of geometric parameters of elliptic slit damper such as strut width, strut height and plate thickness on the seismic performance of the beam-to-column connection. The stress distribution is improved along the struts in the proposed slit damper with elliptic slits and the stress concentration is decreased in the end parts of struts. The average contributions of elliptic slit dampers, beam and other sections to the energy dissipation are about 97.19%, 2.12% and 0.69%, respectively.

Keywords: seismic performance; beam-to-column connections; elliptic slit dampers; geometric parameters

1. Introduction

After the Northridge and Kobe earthquakes, many of the steel structures suffered severe damage and collapse of main structural members. The damages were commonly observed at the connection of structures, such as beam-to-column and bracing joints. Many investigations have been performed in order to solve the problem of low rotational capacity of steel moment connections (Saffari *et al*. 2013). Yielding of metallic materials is one of the most popular passive control mechanisms for dissipating seismic energy (Soong and Spencer 2002, Zhang *et al*. 2015). To improve seismic performance of the connections, numerous metallic devices have been proposed such as the ADAS (Bergman and Goel 1987, Bayat and Bayat 2014), honeycomb damper (Kobori *et al*. 1992), TADAS (Tsai *et al*. 1993), steel shear panel (Nakashima *et al*. 1994, Zahrai 2015), steel slit damper (SSD) (Wada *et al*. 1997), pipe damper (Maleki and Bagheri 2010a, b), U-shaped damper (Tagawa and Gao 2012) and dual pipe damper (Maleki and Mahjoubi 2013). Slit damper is a plate or a standard section with a number of slits in its web. The remaining struts in the web of the damper, dissipate seismic energy with inelastic deformation absorption and also prevent seismic energy transmission to the main structural members. Excellent hysteretic behavior, easy accessibility, simple replacement after earthquake and low fabrication costs are some of advantages of steel slit dampers (Chan and Albermani 2008). Slit devices can be used at different configurations such as bracing joints (Lee *et al*. 2002, Chan and Albermani 2008), beam-to-column connections (Oh *et al*. 2009) and steel slit walls as fuses (Ke and Yam 2016, Ke and Chen 2014).

Wada *et al*. (1997) carried out an experimental study on steel slit damper that slit damper was installed on a bracket on the main frame beam. The results of cyclic loading tests showed that the slit damper had a stable hysteretic curve and a sufficient energy absorption capacity. Lee *et al*. (2002) proposed the use of steel plate slit damper at X-type braced frame to prevent bracing buckling and to absorb seismic input energy. They conducted experimental and theoretical investigations on the ultimate energy absorption capacity of slit damper under shear force. The skeleton part of load-displacement curve was predicted by tri-linear model. It was concluded that steel slit dampers had a stable hysteretic behavior under shear loads. Chan and Albermani (2008) tested nine steel slit dampers under cyclic loading to assess their geometric parameters for maximum energy dissipation. The slit dampers with wider slits were more flexible and those with shorter slits had more stiffness and energy absorption but were fractured earlier than the others. It was found that slit dampers dissipated a considerable amount of energy (6.9-10.3 kJ) and were fractured after cumulative displacement of about 500 mm. Oh *et al*. (2009) proposed the application of slit damper in the beam-to-column connection to overcome brittle failure of moment frame connections. Cyclic tests were performed on three full-scale sub-assemblages equipped with slit dampers and on one Post-Northridge welded connection. The test results demonstrated an excellent hysteretic behavior of their proposed connections. Moreover, plastic deformation

*Corresponding author, Ph.D., Associate Professor,
E-mail: s.r.mousavi@eng.usb.ac.ir
[a] M.S. Student

ISSN: 1229-9367 (Print), 1598-6233 (Online)

localized at the slit dampers while main structural members (column and beam) had an elastic behavior. The average plastic rotation of beam-to-column connections was 0.037 rad and the slit dampers were able to dissipate about 94% of all absorbed energy.

Benavent-Climent (2010) tested a tube-in-tube brace damper consists of two hollow sections, where the outer hollow section had a series of slits through its wall. The test results showed that the damper exhibited remarkable energy dissipation capacity and stable hysteretic behavior. Furthermore, a hysteretic model has been presented to predict the ultimate energy dissipation capacity of the damper. The shape of slit dampers presented by Chan and Albermani (2008) has been optimized by Ghabraie *et al*. (2010) using modified BESO algorithm. Total plastic energy dissipation was maximized to reach a high energy dissipation per unit volume. It was concluded that optimized shape of slit damper dissipated 37% more energy compared to the former specimen. Karavasilis *et al*. (2012) developed a minimal-damage seismic design approach for steel buildings using slit dampers in parallel to viscous dampers. It was observed that residual drifts and peak total floor accelerations of the steel MRF with slit devices and viscous dampers were lower than those of the conventional MRF. Thus, the MRF with slit devices and viscous dampers were suffered less damage compared to the conventional MRF. Safari *et al*. (2013) conducted a parametric study to figure out the best configuration of slit dampers with respect to different beam length-beam depth ratios. They used steel slit dampers as energy dissipation element to increase the ductility of beam-to-column connections. Their suggested connections was intended to cause a delay in failure using a complicated load transferring system which utilized some additional plates through load transferring path from beam to column.

Koken and Koroglu (2014) performed experimental and theoretical studies on the behavior of beam-to-column connections with slit dampers and compared them with the extended end plate connection. Unlike the extended end plate connection, the connections equipped with slit dampers demonstrated a good hysteretic performance without sustaining any damage to the beam and column. Lima *et al*. (2015) studied the behavior of steel slit devices which were utilized as a link in eccentric bracings for seismic retrofitting of RC frames. Nonlinear time history analyses of an existing RC frame with the mentioned bracings have been carried out by taking into account the low-cycle fatigue. It was found that the top displacement demand of the structure was effectively decreased by using the slit devices. Lee and Kim (2015) investigated the seismic performance of hybrid slit-friction dampers by nonlinear dynamic analysis. The analysis results demonstrated that the damage and residual displacements of main structural members are decreased in the structure equipped with hybrid passive dampers. Hedayat (2015) performed a parametric study to predict the force-displacement behavior of unbuckled slit dampers with different types and geometries. For this purpose, he suggested some formulas for each type of slit dampers based on the finite element results. Tagawa *et al*. (2016) proposed a seesaw energy dissipation system equipped with steel slit dampers in order to remain the bracing members in tension state and to improve damper stiffness and energy dissipation characteristics. They presented the lateral story stiffness and strength formulas for the mentioned system. In addition, a tri-linear model has been introduced to predict the cyclic behavior of the system.

With reviewing the previous investigations, it was observed that the use of steel slit dampers with uniform strut width resulted in stress concentration at the end parts of the damper struts and unbalanced distribution of von-Mises stresses along the struts. Furthermore, slit dampers were commonly fractured in the end parts of its struts. This may be due to the low participation of the struts middle parts in the energy dissipation. Thus, in the present study elliptic steel slit damper (ESSD) is proposed in such a way that the end parts of struts have more energy absorption area than the struts middle parts. Also, the effect of geometric parameters of elliptic slit damper is investigated on the seismic performance of the beam-to-column connection. So, different values of strut width, strut height and plate thickness of the elliptic slit damper are considered in the analyses modeled in ABAQUS (2010) finite element software.

2. Device design

According to the previous studies, the analytical yielding strength (p_y) and apparent maximum strength (p_u) of the slit damper can be achieved as follows (Lee *et al*. 2002, Oh *et al*. 2009)

$$p_y = \min\left\{ n\frac{F_y t B^2}{2H'}, n\frac{2F_y tB}{3\sqrt{3}} \right\} \tag{1}$$

$$p_u = \min\left\{ n\frac{F_u t B^2}{2H'}, n\frac{2F_u tB}{3\sqrt{3}} \right\} \tag{2}$$

where n, t, B, H', F_y and F_u are number of struts, thickness of the plate, struts width, equivalent height of the struts, yield stress and maximum stress of steel material, respectively. By using some simplifications, the effective width of elliptic slit damper (B_{eff}) is defined as follows:

$$B_{eff} = B - \frac{B}{r} \tag{3}$$

where r is the minor radius of elliptic slit. By substituting the effective width (B_{eff}) and total height of struts (H_T) in Eqs. (1) and (2), the analytical yielding strength (P_y) and apparent maximum strength (P_u) of the elliptic slit damper are given by

$$P_y = \min\left\{ n\frac{F_y t {B_{eff}}^2}{2H_T}, n\frac{2F_y tB_{eff}}{3\sqrt{3}} \right\} \tag{4}$$

$$P_u = \min\left\{ n\frac{F_u t {B_{eff}}^2}{2H_T}, n\frac{2F_u tB_{eff}}{3\sqrt{3}} \right\} \tag{5}$$

Considering the effective width of elliptic slit damper, the yield displacement is expressed as (Chan and Albermani 2008)

$$\delta_y = \frac{0.5\varepsilon_y H_T^2}{B_{eff}} \tag{6}$$

where ε_y is the yield strain of the steel material. So, the lateral stiffness of the elliptic slit damper (K_{damper}) can be calculated by

$$K_{damper} = \frac{P_y}{\delta_y} \tag{7}$$

3. Modeling methodology and verification

Experimental specimens D1 and D2 tested by Oh *et al*. (2009) are modeled to verify the accuracy of finite element modeling in ABAQUS software. The test specimens were beam-to-column connections consisted of a wide flange beam (H-582×302×12×17), a column (H-400×400×21×21), two slit dampers and some other parts, as shown in Fig. 1. Cyclic loading protocol is applied based on the yield rotation corresponding to the plastic moment of the beam, as mentioned by Oh *et al*. (2009). The distance between the loading point and the column center was 3500 mm. Shell elements are used to model damper, beam, column and column stiffener while split-T and damper-beam bottom flange connecting plate are modeled using solid elements. The modulus of elasticity of steels is considered 193 GPa and 214 GPa for damper plate and other sections, respectively. The density and Poisson ratio of steels are assumed 7850 kg/m^3 and 0.3, respectively.

The effects of geometric nonlinearity (large displacement and strain formulations) and material nonlinearity are considered in the model. As indicated in Fig. 2 and Table 1, steel nonlinear properties of slit dampers and other sections are defined with completed and bilinear stress-strain curves, respectively. The plasticity behavior of steel materials is based on the von-Mises yielding criteria and the associated flow rule.

The pin boundary conditions are determined at the both ends of column to simulate the behavior of a moment resisting frame. The interaction between different surfaces is defined by tie constraints such that the connected surfaces have the same displacement (ABAQUS/CAE User's Manual 2010). A total of 15 surface pairs are included in the finite element model. All the parts of connection are separately discretized into standard linear mesh. The element types of S4R (four-node shell element with reduced integration) and C3D8R (eight-node brick solid element with reduced integration) are used for the shell and solid elements, respectively. All the parts at the connection region are modeled with a finer mesh to achieve more accuracy. Mesh sensitivity analysis is performed to specify the suitable mesh density of different parts. Fig. 3 shows the mesh density of the finite element model which was tested by Oh *et al*. (2009). The entire model of each specimen included approximately 14,000 elements.

As observed in Fig. 4, the skeleton curves obtained from finite element modeling have a good agreement with

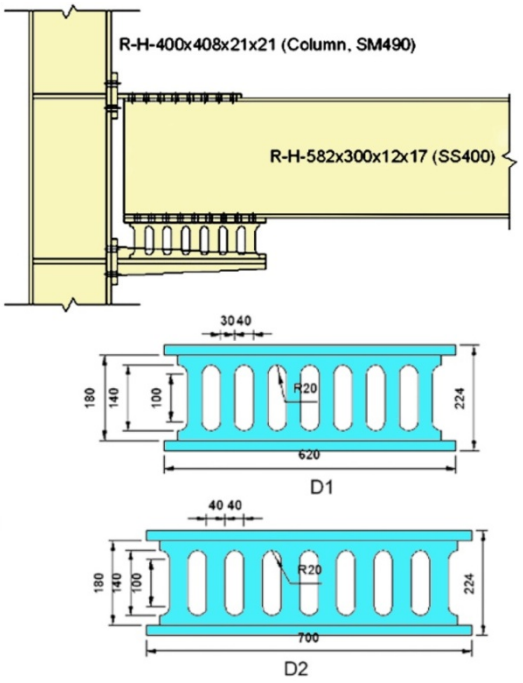

Fig. 1 Beam-to-column connection equipped with D1 and D2 slit dampers presented by Oh *et al*. (2009)

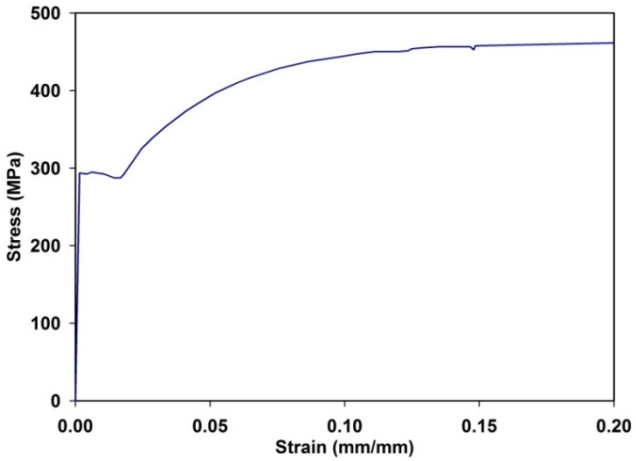

Fig. 2 Stress-strain curve of steel material used for slit damper (Oh 1998)

Table 1 Mechanical properties of steel materials (Oh 1998)

Section	F_y (MPa)	F_u (MPa)	Elongation (%)
Beam's web	332.66	478.50	26.63
Beam's flange	312.09	471.21	29.60
Damper	287.07	454.69	29.80
Column's flange	309.60	450.77	30.73
Column's web	335.17	461.46	25.91

experimental ones presented by Oh *et al*. (2009) for specimens D1 and D2. The average error of about 3.4% and 3.1% is observed for analytical results of specimens D1 and D2, respectively.

The distribution of von-Mises stresses of specimens D1

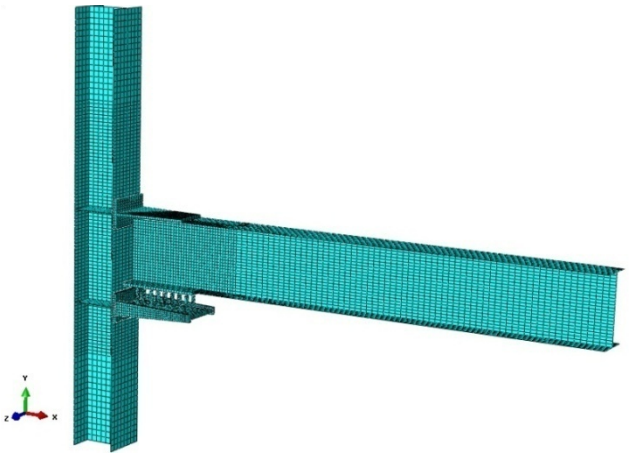

Fig. 3 Mesh density of finite element model of specimen D1

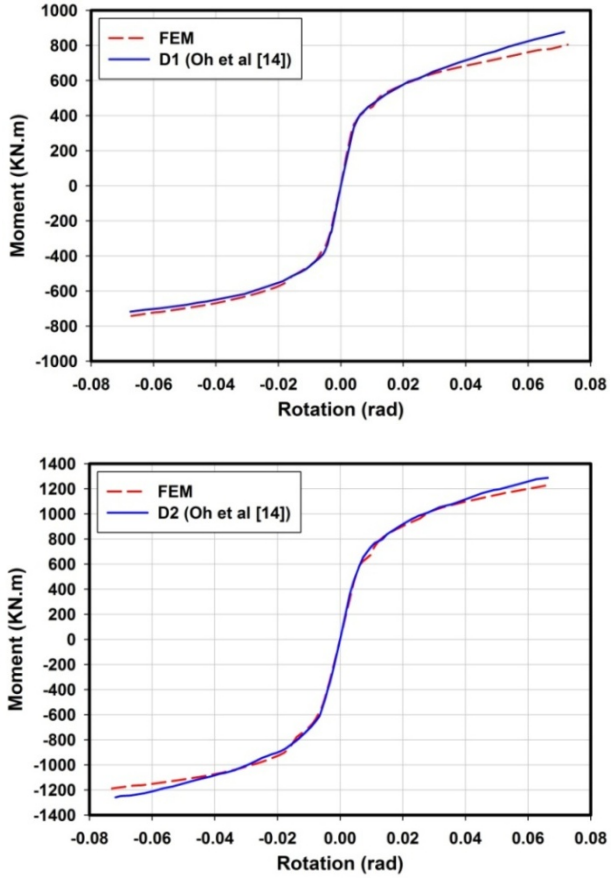

Fig. 4 Comparison between analytical and experimental skeleton curves of specimens D1 and D2

and D2 just before failure is illustrated in Fig. 5. It can be seen that the stress concentration occurs at the end parts of the damper struts, which it complies well with experimental observations reported by Oh *et al* (2009).

The beam-to-column connections equipped with elliptic slit dampers are modeled in the ABAQUS finite element software to evaluate the effects of geometric parameters on the behavior of the connection (Fig. 6). Cyclic loading protocol is exerted on the beam according to the FEMA-350 (2000). The details of elliptic slit dampers with different

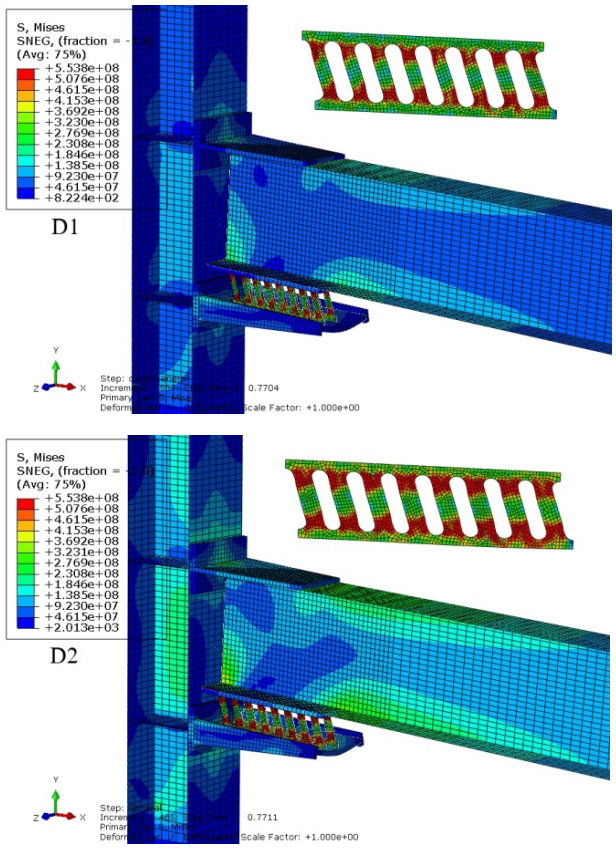

Fig. 5 von-Mises stress contours for specimens D1 and D2

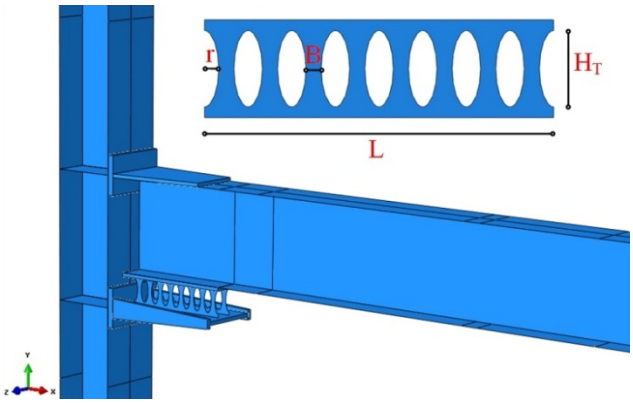

Fig. 6 Modeling of beam-to-column connection equipped with elliptic slit dampers

strut width, strut height and plate thickness are summarized in Tables 2, 3 and 4, respectively, where B is struts width, r is minor radius of elliptic slit, L is damper length and H_T is total height of struts.

4. Discussion of results

4.1 Effect of damper strut width on the behavior of the connection

The von-Mises stress contours of the connection for different strut widths of elliptic slit damper just before failure are shown in Fig. 7. The distribution of stresses at

Table 2 Geometry of the elliptic slit dampers with different strut widths

Specimen	B (mm)	r (mm)	H_T (mm)	L (mm)	t (mm)	B/t	Bt/H_T (mm)
ESSD1	32	24	140	640	19	1.68	4.34
ESSD2	28	26	140	640	19	1.47	3.80
ESSD3	24	28	140	640	19	1.26	3.26
ESSD4	20	30	140	640	19	1.05	2.71

Table 3 Geometry of the elliptic slit dampers with different strut heights

Specimen	B (mm)	r (mm)	H_T (mm)	L (mm)	t (mm)	B/t	Bt/H_T (mm)
ESSD5	32	24	120	640	19	1.68	5.07
ESSD1	32	24	140	640	19	1.68	4.34
ESSD6	32	24	160	640	19	1.68	3.80
ESSD7	32	24	180	640	19	1.68	3.38

Table 4 Geometry of the elliptic slit dampers with different plate thicknesses

Specimen	B (mm)	r (mm)	H_T (mm)	L (mm)	t (mm)	B/t	Bt/H_T (mm)
ESSD8	32	24	140	640	14	2.29	3.20
ESSD9	32	24	140	640	16	2.00	3.66
ESSD1	32	24	140	640	19	1.68	4.34
ESSD10	32	24	140	640	22	1.45	5.03

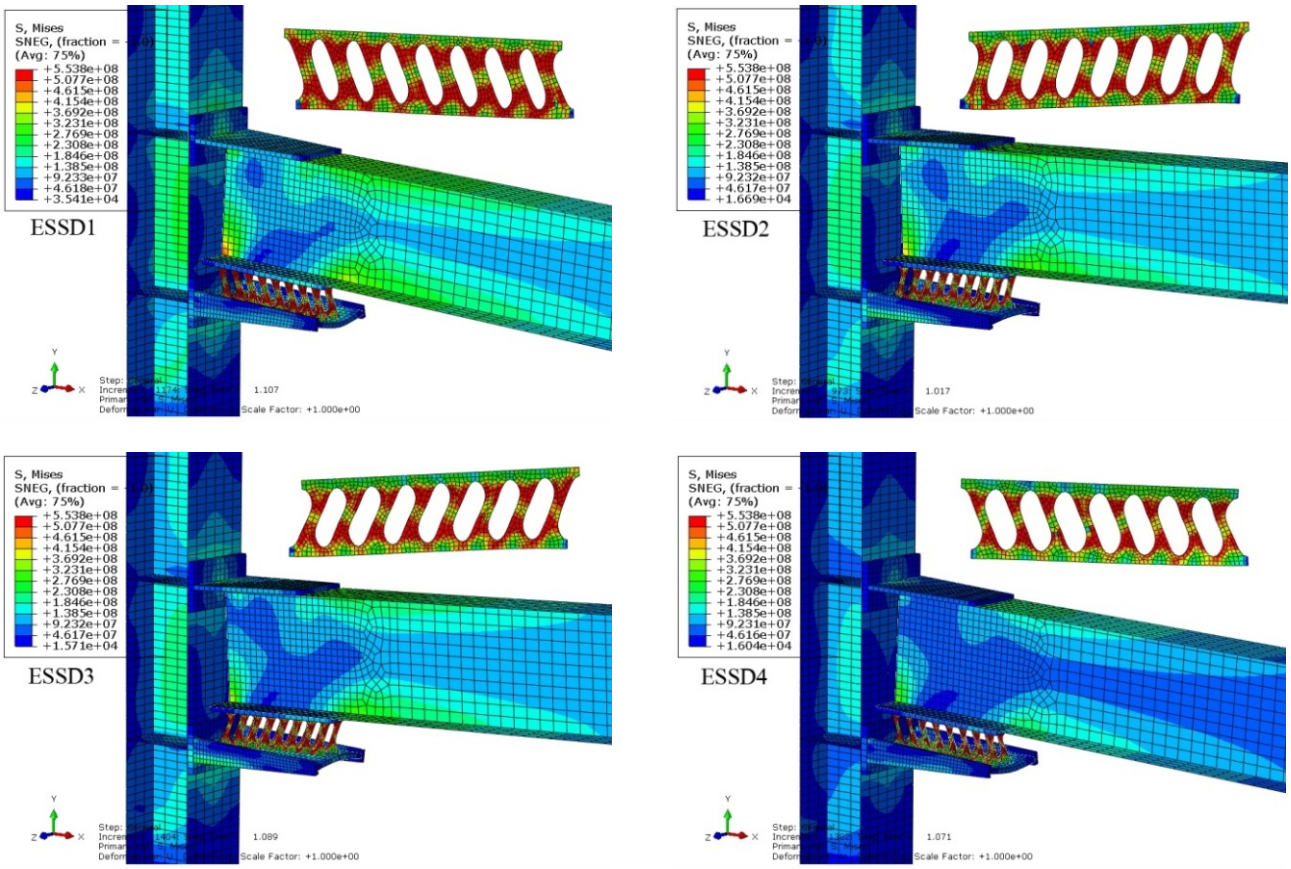

Fig. 7 von-Mises stress contours of connections with different strut widths of elliptic slit damper

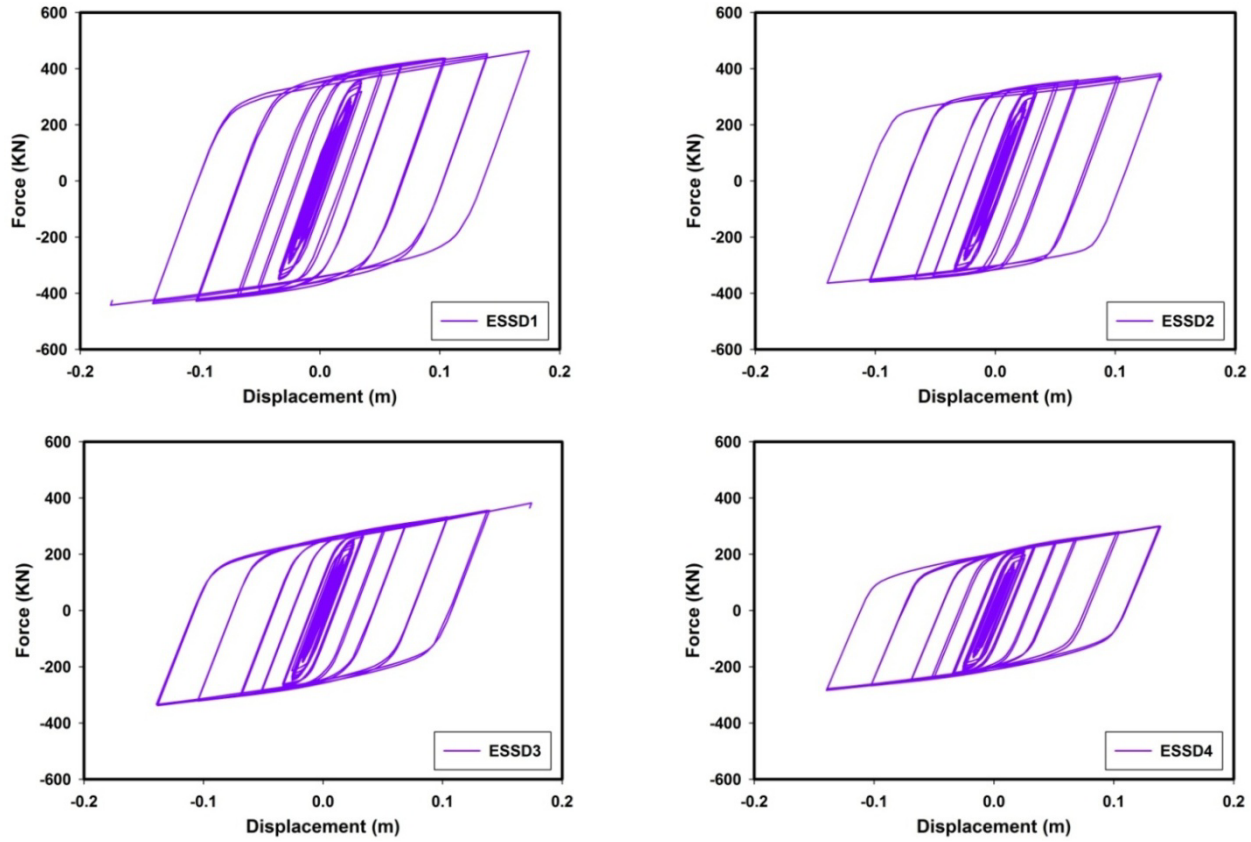

Fig. 8 Force-displacement curves of connections with different strut widths of elliptic slit damper

the main structural members is reduced with decrease of damper strut width. Consequently, the stress concentration is increased at the elliptic slit dampers. Specimen ESSD1 (having elliptic slit dampers with wider struts) experiences the highest level of stresses at the panel zone compared to the other specimens. However, the panel zone of all the specimens remains in the elastic state. Furthermore, in the specimen ESSD1, stress concentration occurs at the bottom corner of the beam web. It can be seen in Fig. 7 that a decrease in the strut width of elliptic slit dampers leads to increasing the contribution of the middle parts of the struts to stress suffering and better stress distribution along the struts.

Fig. 8 shows the force-displacement hysteretic curves for specimens ESSD1 to ESSD4. All the specimens have plump hysteretic loops indicating that the elliptic slit dampers have a good hysteretic behavior. A negligible amount of strength degradation appears at the last loading cycles for specimens ESSD1 and ESSD2. According to Fig. 8, decreasing the strut width of damper decreases the maximum force suffered by the beam-to-column connection. Energy dissipation capacity is one of the substantial seismic features of any structure which can be achieved from the area within the force-displacement loop. The amounts of energy dissipated by the specimens ESSD1 to ESSD4 are 167.81 kJ, 132.20 kJ, 112.42 kJ and 94.59 kJ, respectively.

The moment-rotation hysteretic curves of specimens ESSD1 to ESSD4 are illustrated in Fig. 9. The maximum moment of specimen ESSD1 exceeded the beam plastic moment (1260 KN.m) which leads to damage occurrence at the beam. While, other elliptic slit dampers having lower strut width experience a moment under the beam plastic moment. The maximum rotational capacities suffered by the connections ESSD1 to ESSD4 are 0.057 rad, 0.045 rad, 0.056 rad and 0.045 rad, respectively. Based on the Figs. 7-9, considering that the damage not be transmitted to the main structural members, specimen ESSD2 has a better seismic performance than the others.

4.2 Effect of damper strut height on the behavior of the connection

Fig. 10 presents the von-Mises stress contours of the connection for different heights of elliptic slit damper just before failure. It can be seen that increasing the damper height leads to decrease of the stress distribution in the main structural members. In the taller dampers, the middle parts of struts undergo a little portion of stresses and the stress concentration is localized at the end parts of damper struts. The highest level of stresses at the panel zone is observed in the specimen ESSD5 (the specimen with the lowest height of damper struts) than the others. However, the panel zone of all the specimens behaves elastically. As illustrated in Fig. 10, stress concentration at the bottom corner of the beam web is reduced with increasing the damper height.

The force-displacement hysteretic curves of connections for various heights of elliptic slit damper are shown in Fig. 11. The hysteretic loops of all the specimens are plump except for the specimen ESSD5, which behaves in a brittle

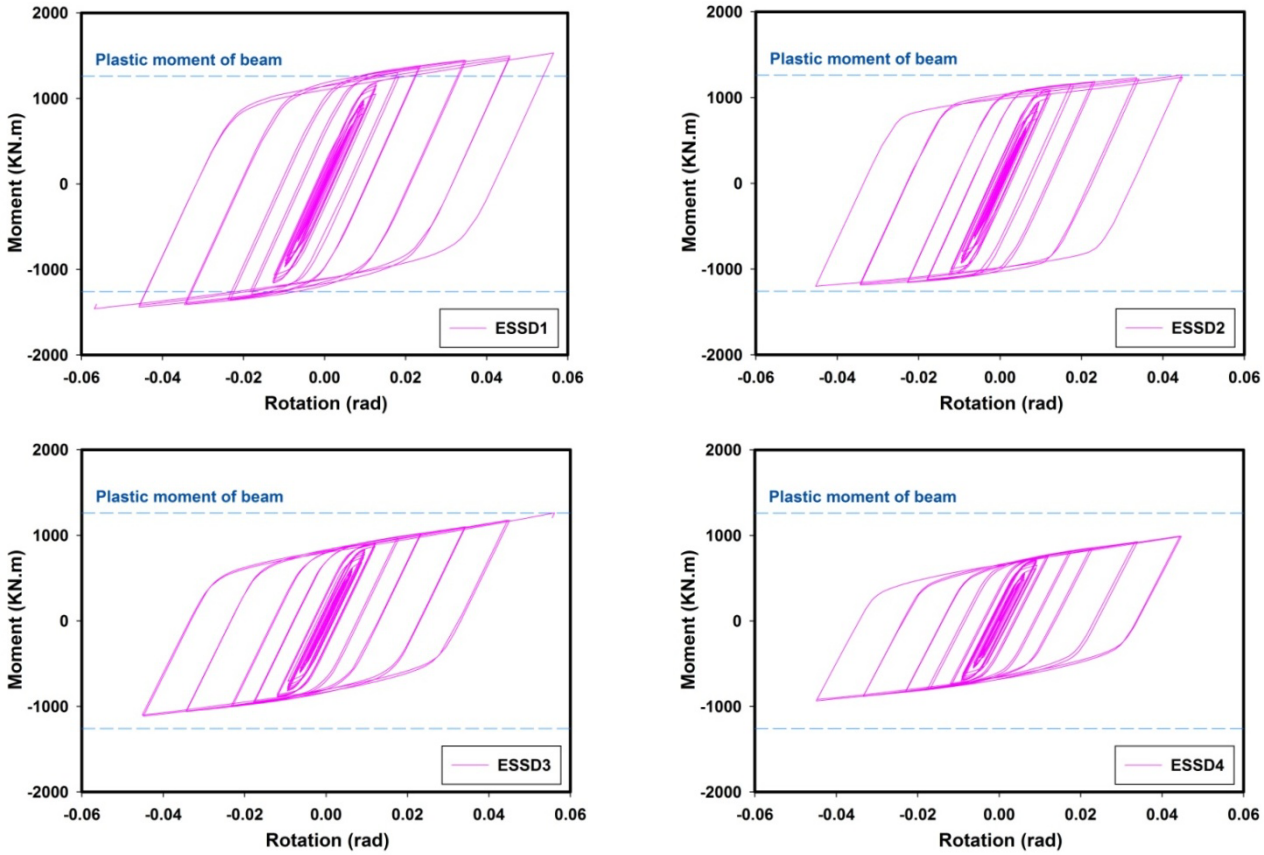

Fig. 9 Moment-rotation curves of connections with different strut widths of elliptic slit damper

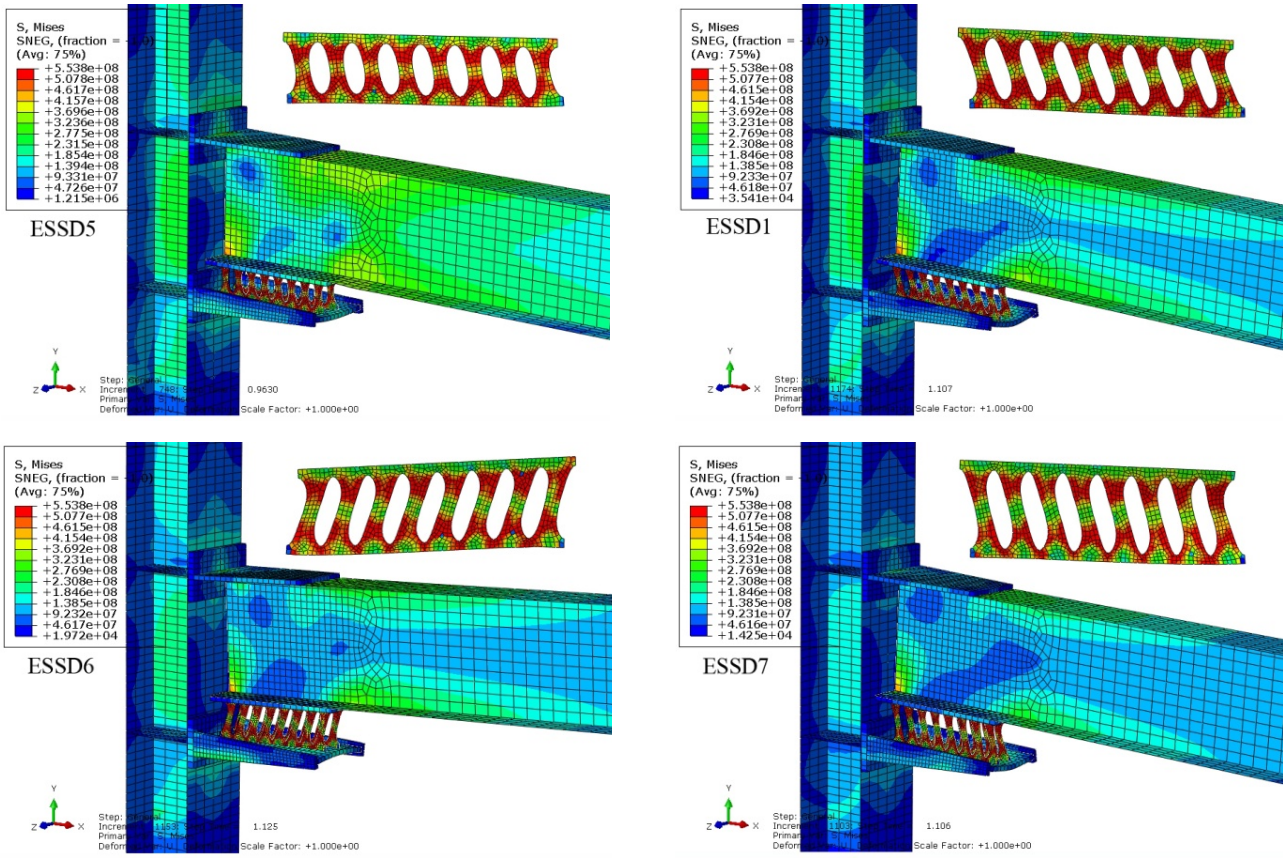

Fig. 10 von-Mises stress contours of connections with different heights of elliptic slit damper

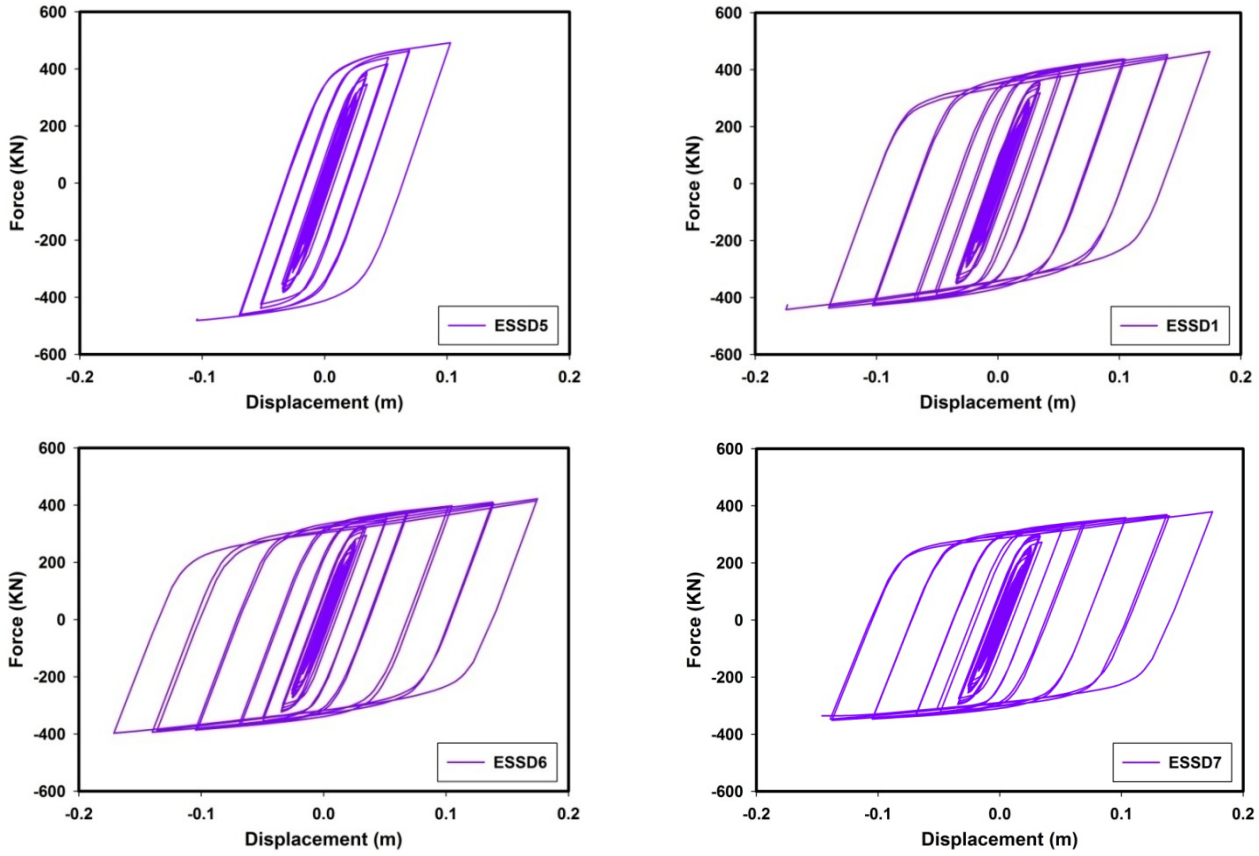

Fig. 11 Force-displacement curves of connections with different heights of elliptic slit damper

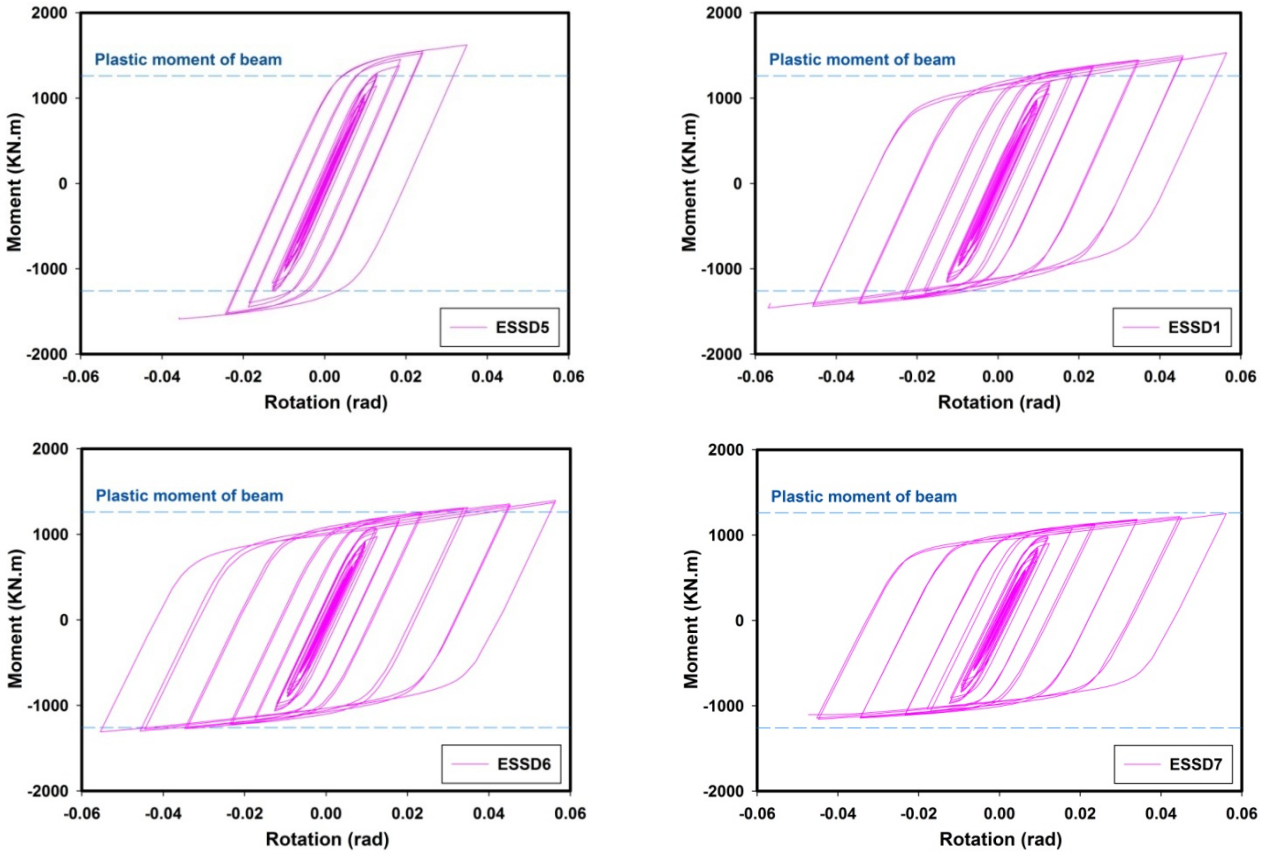

Fig. 12 Moment-rotation curves of connections with different heights of elliptic slit damper

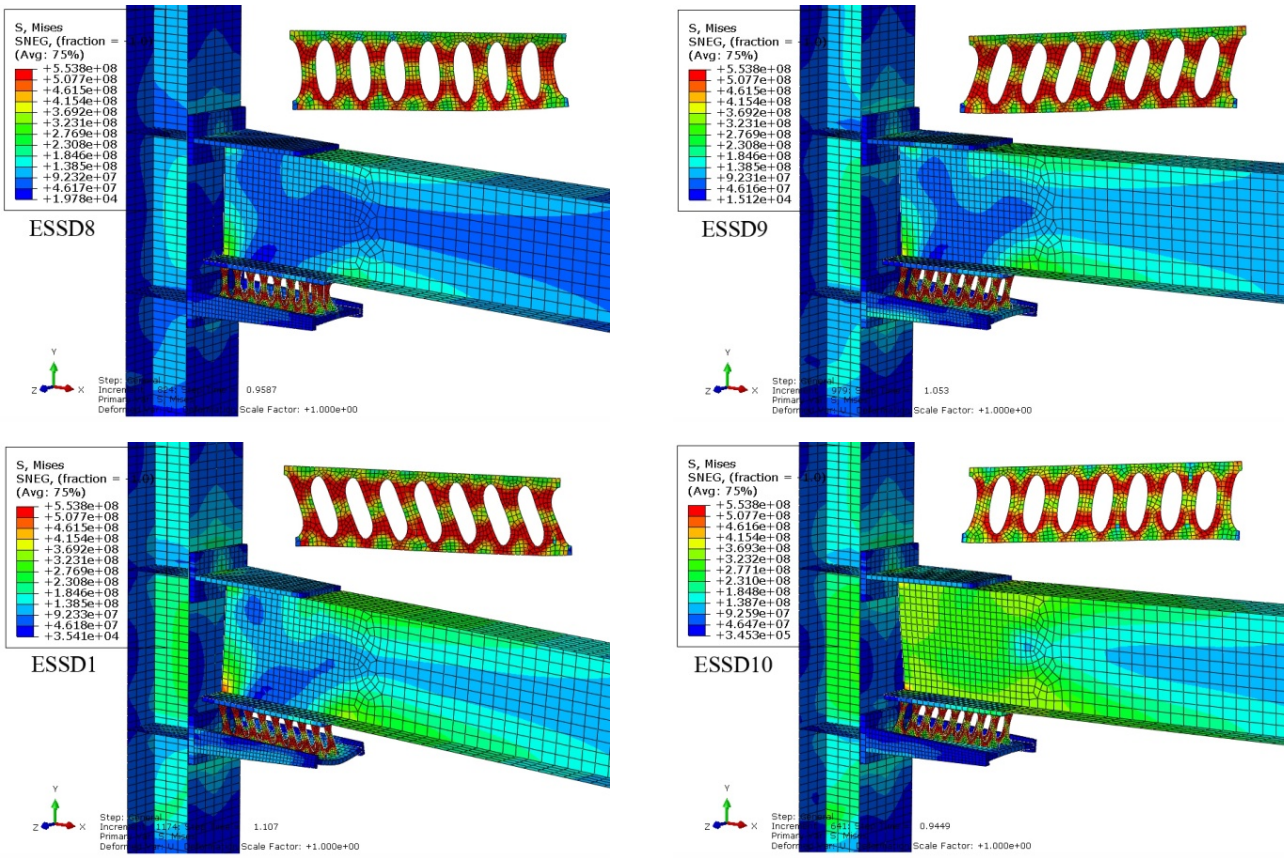

Fig. 13 von-Mises contours of connections with different plate thicknesses of elliptic slit damper

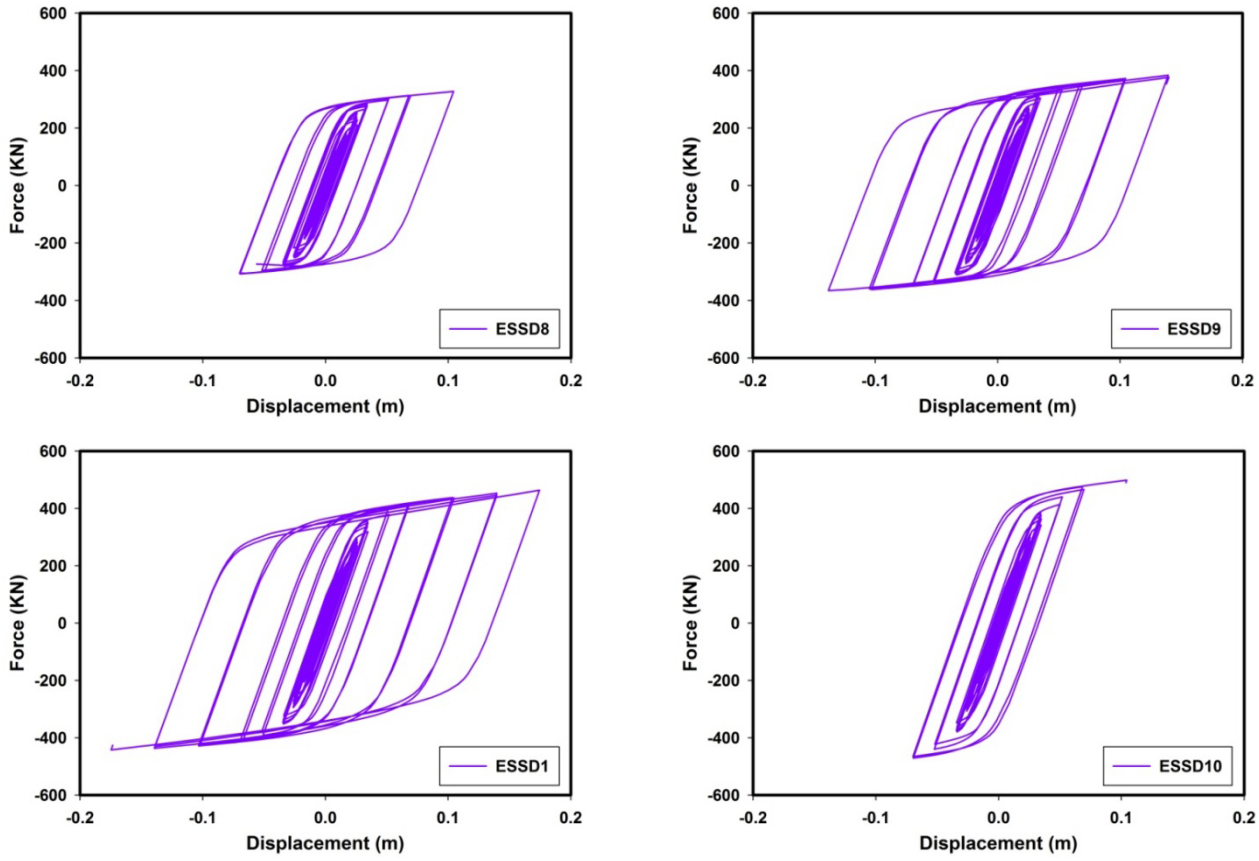

Fig. 14 Force-displacement curves of connections with different plate thicknesses of elliptic slit damper

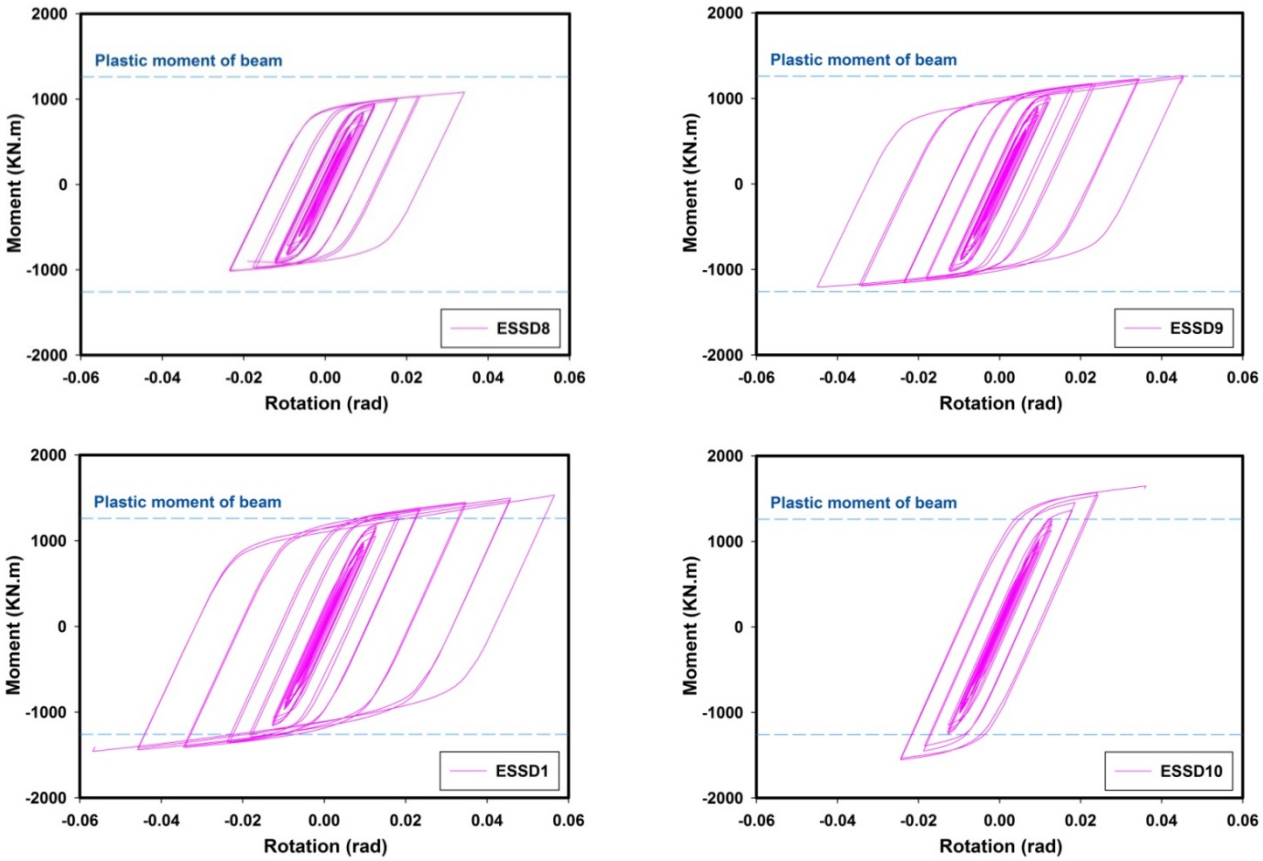

Fig. 15 Moment-rotation curves of connections with different plate thicknesses of elliptic slit damper

manner due to its short-height dampers. Specimens ESSD1, ESSD2 and ESSD3 have inconsiderable strength degradation at the last loading cycles. As this figure shows, an increase in the height of elliptic slit dampers results in a slightly reduction of the maximum force suffered by the connections. The amounts of energy dissipation of specimens ESSD5, ESSD1, ESSD6 and ESSD7 are 82.15 kJ, 167.81 kJ, 175.11 kJ and 145.86 kJ, respectively.

Fig. 12 presents the moment-rotation curves of connections for different heights of elliptic slit damper. It can be seen that, all the specimens experience a higher moment than the beam plastic moment except for the specimen ESSD7. The maximum rotational capacities for the connections ESSD5, ESSD1, ESSD6 and ESSD7 are 0.036 rad, 0.057 rad, 0.056 rad and 0.056 rad, respectively. According to Figs. 10-12, with respect to taking no damage in the main structural members, specimen ESSD7 has a better seismic performance compared to the others.

4.3 Effect of damper plate thickness on the behavior of the connection

The von-Mises stress contours of connection for different plate thicknesses of elliptic slit damper just before failure are illustrated in Fig. 13. The stress distribution in the beam and column shows an increase, as the thickness of damper plate increases. Specimen ESSD10 which has the thickest damper plate experienced the highest level of stresses at the panel zone compared to the others. However, the panel zone of all the specimens stays in the elastic range. The stress concentration is observed at the top and bottom corners of the beam web for specimen ESSD10. Local buckling and out of plane deformations occur in the specimens ESSD8 (the specimen with the thinnest damper plate) and ESSD10 (the specimen with the thickest damper plate), respectively. It can be concluded from Fig. 13 and Table 4 that the specimen ESSD8 in which the strut width-to-thickness ratio (b/t) of elliptic slit damper is greater than 2, experience local buckling at the damper strut, where it conforms to the finding reported by Hedayat (2015).

Fig. 14 presents the force-displacement curves of connections for various plate thicknesses of elliptic slit damper. Increase of the plate thickness leads to increasing of the maximum force suffered by the connections, although the hysteretic behavior was not desirable in the connection with the thickest damper plate, since specimen ESSD10 is not capable to supply sufficient ductility due to premature failure of the connection. Specimens ESSD8, ESSD9, ESSD1 and ESSD10 dissipate 66.44 kJ, 130.31 kJ, 167.81 kJ and 53.13 kJ of energy, respectively.

The moment-rotation curves of connections for different plate thickness of elliptic slit damper are shown in Fig. 15. Unlike the specimens ESSD 1 and ESSD 10, specimens ESSD8 and ESSD9 having a thinner damper plate experience a moment lower than the beam plastic moment. The excessive increase in the plate thickness of the damper (specimen ESSD10) leads to premature failure of the beam-to-column connection in the primary stages of loading

cycles. The maximum rotational capacities suffered by the connections ESSD8, ESSD9, ESSD1 and ESSD10 are 0.034 rad, 0.045 rad, 0.057 rad and 0.036 rad, respectively. It can be concluded from Figs. 13-15, with respect to taking no damage in the main structural members, specimen ESSD9 has a better seismic performance than the others.

4.4 Comparison of skeleton curves for specimens

The hysteretic and ductility characteristics of beam-to-column connection with various types of elliptic slit dampers can be compared effectively in the skeleton curves. The maximum moment of specimens ESSD1, ESSD5, ESSD6 and ESSD10 exceed the beam plastic moment. This is due to wider struts of damper in specimen ESSD1, shorter height of damper in specimens ESSD5 and ESSD6 and thicker plate of damper in specimen ESSD10. It is observed that specimens ESSD1, ESSD3, ESSD6 and ESSD7 exhibit more rotational capacity than the other specimens. Specimen ESSD8 sustains the lowest rotational capacity, where thin damper plate results in local buckling and soon failure of the connection. Moreover, the rotational capacities of specimens ESSD5 and ESSD10 are not desirable because of shorter height and thicker plate of the damper, respectively. The average rotational capacity of all the connections is about 0.047 rad. Generally, most of connections equipped with elliptic slit dampers are reached to 0.04 rad rotation. So, they satisfy the requirements for special moment frame connections (AISC 2005). It can be concluded from Tables 2-4 and Fig. 16 that beam-to-column connections experience brittle failure and low rotational capacity when the parameter Bt/HT of elliptic slit damper was greater than 5 (as observed in specimens ESSD5 and ESSD10). These problems occur due to the excessive stiffness of such dampers.

4.5 Comparison of equivalent damping ratio for specimens

Equivalent damping ratio (ξ_{eq}) for the specimens is calculated from the force-displacement hysteretic curves (see Fig. 17), as expressed in Eq. (8)

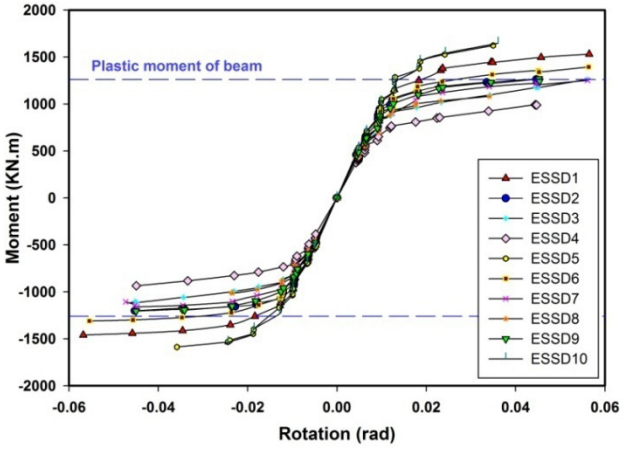

Fig. 16 Skeleton curves of elliptic slit dampers with different geometries

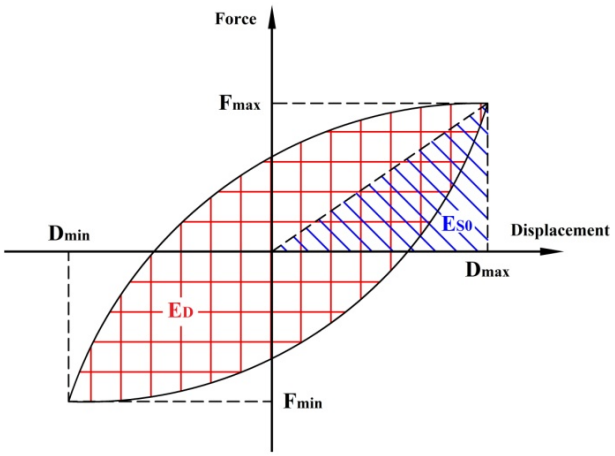

Fig. 17 Definition of dissipated energy and equivalent elastic energy

$$\xi_{eq} = \frac{E_D}{4\pi E_{S0}} \tag{8}$$

where E_D is dissipated energy in the last loading cycle which can be achieved from the area within the closed hysteretic loop, as shown in Fig. 17.

E_{S0} is equivalent elastic energy which can be calculated using Eq. (9)

$$E_{S0} = \frac{F_{\max} D_{\max}}{2} \tag{9}$$

where $F_{\max}$ and $D_{\max}$ are maximum values of force and displacement during the loading cycle, respectively. The calculated values of dissipated energy, equivalent elastic energy and equivalent damping ratio for different specimens are summarized in Table 4. Specimen ESSD2 has the highest amount of equivalent damping ratio among all the specimens. Furthermore, Specimens ESSD9, ESSD6, ESSD3 and ESSD4 also experience desirable values of equivalent damping ratio. As expected, the lowest amount of equivalent damping ratio is observed in specimens ESSD10 and ESSD5, where the parameter Bt/H_T of elliptic slit damper is greater than 5.

4.6 Contributions of sections to the energy dissipation

Different parts of the beam-to-column connection such as dampers, beam, column and split-T plate participate in the energy dissipation. With respect to that the participation of the dampers and beam in the energy dissipation are greater than that of the other sections, the contributions of the sections are categorized in three groups: beam, dampers and other sections. As illustrated in Fig. 18, elliptic slit dampers of specimens ESSD4, ESSD3 and ESSD2 can effectively contribute to about 99.34%, 99.30% and 99.28% of the total dissipated energy, respectively. The dampers of other specimens also dissipated a considerable amount of the total absorbed energy rather than the beam and other sections. For the specimens ESSD1 to ESSD10, the average contributions of elliptic slit dampers, beam and other

Table 5 Energy quantities and equivalent damping ratio for the specimens

Specimen	E_D (kJ)	E_{SO} (kJ)	ξ_{eq}	Specimen	E_D (kJ)	E_{SO} (kJ)	ξ_{eq}
ESSD1	167.81	40.46	0.33	ESSD6	175.11	36.89	0.38
ESSD2	132.20	26.5	0.40	ESSD7	145.86	33.15	0.35
ESSD3	112.42	24.76	0.36	ESSD8	66.44	17.09	0.31
ESSD4	94.59	20.9	0.36	ESSD9	130.31	26.85	0.39
ESSD5	82.15	25.27	0.26	ESSD10	53.13	26.05	0.16

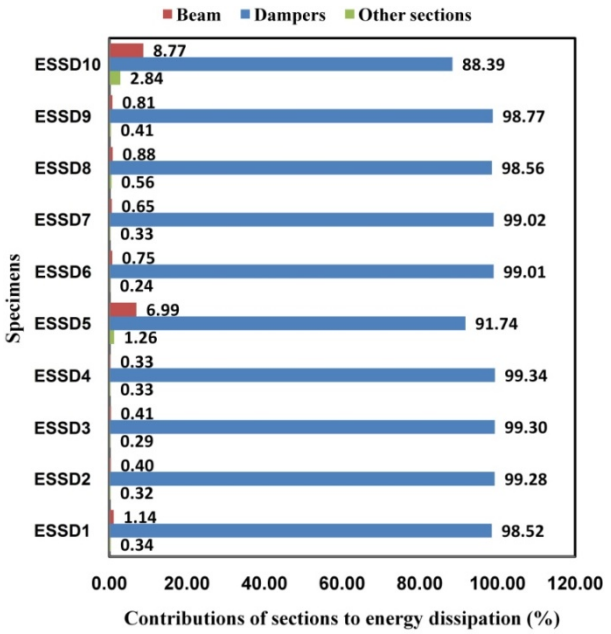

Fig. 18 Contributions of different sections to the energy dissipation

sections to the energy dissipation are about 97.19%, 2.12% and 0.69%, respectively. Therefore, elliptic slit dampers can provide a significant participation in the energy dissipation. It can be seen from Fig. 18 that the portions of dissipated energy by the beam of specimens ESSD10 and ESSD5 are relatively large compared to those of the other specimens due to the thicker plate and shorter height of the damper, respectively. Thus, contribution of the beam section to the energy dissipation increases significantly, when the parameter Bt/H_T of elliptic slit damper is greater than 5.

5. Conclusions

The aim of this paper is to enhance the seismic performance of steel slit dampers in the beam-to-column connection using finite element analysis. Considering the previous investigations, it is observed that slit dampers were commonly fractured in the end parts of struts. This may be due to low participation of the struts middle parts in the energy dissipation. Therefore in this paper, elliptic slit damper is proposed such that the end parts of struts have more energy absorption area than the struts middle parts. The effects of geometric parameters of elliptic slit damper such as strut width, strut height and plate thickness on the seismic behavior of the beam-to-column connection are investigated through a parametric study. Based on the results of analyses, the main following conclusions can be drawn:

- In the proposed slit damper with elliptic slits, the stress distribution is improved along the struts of damper. Furthermore, utilizing the elliptic slits results in more participation of the middle part of struts in the energy dissipation. Consequently, stress concentration is decreased at the end parts of damper struts.
- Decreasing the strut width or plate thickness or increasing the height of elliptic slit dampers leads to decrease of the maximum values of force and moment sustained by the connection. It also results in reduction of von-Mises stress distribution at the main structural members and increment of the stress concentration at the dampers.
- Using thin plates for elliptic slit dampers causes the local buckling and low rotational capacity of the beam-to-column connection. To prevent local buckling from occurring, the strut width-to-thickness ratio (b/t) of elliptic slit damper should not exceed 2.
- The results show that the beam-to-column connections experience brittle failure and low rotational capacity and also low equivalent damping ratio when the parameter Bt/H_T of elliptic slit damper is greater than 5. This is generally due to excessive stiffness of elliptic slit dampers, such as using short-height or thick-plate dampers. However, the other specimens exhibit a favorable hysteretic performance and adequate equivalent damping ratio.
- Elliptic slit dampers can dissipate a significant amount of seismic energy compared to the beam and other sections. For all of the specimens, the average contributions of elliptic slit dampers, beam and other sections to the energy dissipation are about 97.19%, 2.12% and 0.69%, respectively. So, it can be concluded that elliptic slit dampers contribute to the energy dissipation, effectively.

References

ABAQUS, Version 9.10 (2010), Dassault Systemes Simulia Corp., Providence, RI, USA.

ABAQUS/CAE User's Manual (2010), Dassault Systemes Simulia Corp., Providence, RI, USA.

AISC (2005), Seismic Provision for Structural Steel Buildings, American Institute of Steel Construction, Chicago, IL., USA.

Bayat, M. and Bayat, M. (2014), "Seismic behavior of special moment-resisting frames with energy dissipating devices under near source ground motions", *Steel Compos. Struct., Int. J.*, **16**(5), 533-557.

Benavent-Climent, A. (2010), "A brace-type seismic damper based on yielding the walls of hollow structural sections", *Eng. Struct.*, **32**(4), 1113-1122.

Bergman, D.M. and Goel, S.C. (1987), "Evaluation of cyclic testing of steel plate devices for added damping and stiffness", Report No. UMCE87-10.MI; University of Michigan, MI, USA.

Chan, R.W.K. and Albermani, F. (2008), "Experimental study of

steel slit damper for passive energy dissipation", *Eng. Struct.*, **30**(4), 1058-1066.
FEMA-350 (2000), Recommended Seismic Design Criteria for New Steel Moment-Frame Buildings; Federal Emergency Management Agency, Washington, D.C., USA.
Ghabraie, K., Chan, R., Huang, X. and Xie, Y.M. (2010), "Shape optimization of metallic yielding devices for passive mitigation of seismic energy", *Eng. Struct.*, **32**(8), 2258-2267.
Hedayat, A.A. (2015), "Prediction of the force displacement capacity boundary of an unbuckled steel slit damper", *J. Constr. Steel Res.*, **114**, 30-50.
Karavasilis, T.L., Kerawala, S. and Hale, E. (2012), "Hysteretic model for steel energy dissipation devices and evaluation of a minimal-damage seismic design approach for steel buildings", *J. Constr. Steel Res.*, **70**, 358-367.
Ke, K. and Chen, Y. (2014), "Energy-based damage-control design of steel frames with steel slit walls", *Struct. Eng. Mech., Int. J.*, **52**(6), 1157-1176.
Ke, K. and Yam, M.C.H. (2016), "Energy-factor-based damage-control evaluation of steel MRF systems with fuses", *Steel Compos. Struct., Int. J.*, **22**(3), 589-611.
Kobori, T., Miura, Y., Fukusawa, E., Yamada, T., Arita, T., Takenaka, Y., Miyagawa, N., Tanaka, N. and Fukumoto, T. (1992), "Development and application of hysteresis steel dampers", *Proceedings of the 10th World Conference on Earthquake Engineering*, Madrid, Spain, July.
Koken, A. and Koroglu, M.A. (2014), "Experimental study on beam-to-column connections of steel frame structures with steel slit dampers", *J. Perform. Constr. Facil., ASCE*, **29**(2), 04014066.
Lee, J. and Kim, J. (2015), "Seismic performance evaluation of moment frames with slit-friction hybrid dampers", *Earthq. Struct., Int. J.*, **9**(6), 1291-1311.
Lee, M.-H., Oh, S.-H., Huh, C., Oh, Y.-S., Yoon, M.-H. and Moon, T.-S. (2002), "Ultimate energy absorption capacity of steel plate slit dampers subjected to shear force", *Steel Struct.*, **2**(2), 71-79.
Lima, C., Martinelli, E. and Faella, C. (2015), "Cost-competitive steel devices for seismic retrofitting of RC frames: Model identification and nonlinear analysis", *J. Steel Struct. Constr.*, **1**, 104.
Maleki, S. and Bagheri, S. (2010a), "Pipe damper, part I: experimental and analytical study", *J. Constr. Steel Res.*, **66**(8-9), 1088-1095.
Maleki, S. and Bagheri, S. (2010b), "Pipe damper, part II: application to bridges", *J. Constr. Steel Res.*, **66**(8-9), 1096-1106.
Maleki, S. and Mahjoubi, S. (2013), "Dual-pipe damper", *J. Constr. Steel Res.*, **85**, 81-91.
Nakashima, M., Iwai, S., Iwata, M., Takeuchi, T., Konomi, S., Akazawa, T. and Saburi, K. (1994), "Energy dissipation behaviours of shear panels made of low yield steel", *Earthq. Eng. Struct. Dyn.*, **23**(12), 1299-1313.
Oh, S.-H. (1998), "Seismic design of energy dissipating multi-story frame with flexible-stiff mixed type connection", Ph.D. Dissertation; Tokyo University, Japan.
Oh, S.-H., Kim, Y.-J. and Ryu, H.-S. (2009), "Seismic performance of steel structures with slit dampers", *Eng. Struct.*, **31**(9), 1997-2008.
Saffari, H., Hedayat, A.A. and Poorsadeghi Nejad, M. (2013), "Post-Northridge connections with slit dampers to enhance strength and ductility", *J. Constr. Steel Res.*, **80**, 138-152.
Soong, T.T. and Spencer Jr., B.F. (2002), "Supplemental energy dissipation: state-of-the-art and state-of-the-practice", *Eng. Struct.*, **24**(3), 243-259.
Tagawa, H. and Gao, J. (2012), "Evaluation of vibration control system with U-dampers based on quasi-linear motion mechanism", *J. Constr. Steel Res.*, **70**, 213-225.
Tagawa, H., Yamanishi, T., Takaki, A. and Chan, R.W.K. (2016), "Cyclic behavior of seesaw energy dissipation system with steel slit dampers", *J. Constr. Steel Res.*, **117**, 24-34.
Tsai, K., Chen, H., Hong, C. and Su, Y. (1993), "Design of steel triangular plate energy absorbers for seismic-resistant construction", *Earthq. Spectra*, **9**(3), 505-528.
Wada, A., Huang, Y.H., Yamada, T., Ono, Y., Sugiyama, S., Baba, M. and Miyabara, T. (1997), "Actual size and real time speed tests for hysteretic steel damper", *Proceedings of Stessa*, Kyoto, Japan, August, pp. 778-785.
Zahrai, S.M. (2015), "Cyclic testing of chevron braced steel frames with IPE shear panels", *Steel Compos. Struct., Int. J.*, **19**(5), 1167-1184.
Zhang, C., Zhou, Y., Weng, D.G., Lu, D.H. and Wu, C.X. (2015), "A methodology for design of metallic dampers in retrofit of earthquake-damaged frame", *Struct. Eng. Mech., Int. J.*, **56**(4), 569-588.

CC